Vacuum-ultraviolet mass-analyzed threshold ionization spectra of iodobutane isomers: Conformer-specific ionization and ion-core dissociation followed by ionization

ARTICLE *in* THE JOURNAL OF CHEMICAL PHYSICS · AUGUST 2001

Impact Factor: 2.95 · DOI: 10.1063/1.1386786

3 AUTHORS, INCLUDING:

Sang Tae Park
Integrated Dynamic Electron Solutions, Inc.
39 PUBLICATIONS **750** CITATIONS

Vacuum-ultraviolet mass-analyzed threshold ionization spectra of iodobutane isomers: Conformer-specific ionization and ion-core dissociation followed by ionization

Sang Tae Park, Sang Kyu Kim,[a] and Myung Soo Kim[b]
National Creative Research Initiative for Control of Reaction Dynamics and School of Chemistry, Seoul National University, Seoul 151-742, Korea

(Received 30 April 2001; accepted 30 May 2001)

Mass-analyzed threshold ionization (MATI) spectra using coherent vacuum ultraviolet radiation have been obtained for *t*-butyl iodide, *iso*-butyl iodide, 2-iodobutane, and 1-iodobutane. The ionization energy to the lower spin–orbit state of *t*-butyl iodide ion has been determined to be 8.9984 ± 0.0006 eV, while the threshold for fragmentation to $t\text{-}C_4H_9^+$ and I has been estimated to be 9.1762 ± 0.0047 eV. Heat of formation of *t*-butyl cation, $\Delta_f H^0(t\text{-}C_4H_9^+)$, has been re-estimated, 733.7 ± 3.3 kJ mol^{-1}. Peaks due to two different conformers of *iso*-butyl iodide ion, P_H and P_C, are clearly resolved in the MATI spectra, enabling the measurement of ionization energies to the lower spin–orbit states of respective conformers, 9.1725 ± 0.0006 and 9.1972 ± 0.0006 eV. Corresponding values for the upper spin–orbit states have been determined from the MATI spectra for the $C_4H_9^+$ fragments generated by dissociation in the ion core of neutral as 9.7394 ± 0.0024 and 9.7649 ± 0.0023 eV. Only two out of three possible 2-iodobutane conformers have been observed in the MATI spectra with ionization energies to their lower spin–orbit states of 9.0883 ± 0.0006 and 9.0913 ± 0.0006 eV, even though conformer identification was not possible. Similarly, it is likely that four distinct peaks observed in the ionization threshold region of the MATI spectra of 1-iodobutane are the origins for the different conformers. Plausible mechanisms for the ion-core fragmentation of iodobutanes are discussed. © *2001 American Institute of Physics.*
[DOI: 10.1063/1.1386786]

I. INTRODUCTION

Zero electron kinetic energy (ZEKE) states live quite long so that delayed pulsed-field ionization of these states generates highly resolved spectra of ions.[1–5] Conventionally, it is called ZEKE spectra when electrons ejected by pulsed-field ionization from long-lived ZEKE states are detected, while detection of the corresponding ions gives mass-analyzed threshold ionization (MATI) spectra.[6,7] Both ZEKE and MATI spectra, when they are obtained by the combined use of molecular beam and high resolution lasers, usually provide accurate and precise values for ionization energies, vibrational frequencies, and even rotational constants of ions in some cases. In this work, we adopt one-photon MATI spectroscopy using a vacuum-ultraviolet (VUV) laser source generated by four-wave mixing in Kr gas.[8,9] Though ZEKE spectroscopy is more advanced in terms of sensitivity and spectral resolution, MATI has some advantages over ZEKE especially in the study of reaction dynamics occurring in ion cores because of the inherent capability of MATI to determine the mass of the chemical species involved.[7] Compared to multi-photon MATI, one-photon VUV MATI[5,10] is not only universal in its application but also straightforward in spectral interpretation since any complication associated with the multi-photon effect can be avoided.

MATI spectroscopic studies of alkyl halide ions have been found to be extremely useful for the accurate determination of important thermodynamic quantities such as heats of formation of alkyl ions and proton affinities of various hydrocarbons.[10] Compared to the more traditional spectroscopic tools such as the measurement of photoionization efficiency (PIE), photoelectron spectroscopy (PES), and photoelectron-photoion coincidence (PEPICO) technique, MATI provides more precise and probably more accurate values of ionization energies and fragmentation thresholds. Thus, related thermodynamic quantities previously estimated from PIE, PES, or PEPICO of alkyl halides can be further refined by MATI spectroscopy of the same molecules.

Recently, our group has reported one-photon VUV MATI spectra of 1- and 2-iodopropane ions.[10] Interestingly, *gauche* and *anti* (or *trans*) conformers of 1-iodopropane were well separated as two distinct peaks in MATI spectra, which resulted in conformer-specific ionization energies. Information on the threshold energies and dynamics involved in the fragmentation of 1- and 2-iodopropane ions has also been obtained from the MATI spectra recorded by detecting parent or fragment ions. In the present work, we have extended the VUV MATI spectroscopic study to various isomers of iodobutanes: *t*-butyl iodide, *iso*-butyl iodide, 2-iodobutane, and 1-iodobutane. Accurate energetics data associated with ionization and ion-core fragmentation of these molecules are reported with discussion about plausible reaction mechanisms therein.

[a]Permanent address: Department of Chemistry, Inha University, Inchon 402-751, Korea.
[b]Author to whom correspondence should be addressed.

TABLE I. Ionization (IE) and appearance (AE) energies of iodobutanes, in eV.

	t-	*iso*-	2-	1-	Ref.
IE($\tilde{X}_1$)[a]	8.9984±0.0006	9.1725±0.0006[b]	9.0883±0.0006[d]	9.2081±0.0006[d]	this work
		9.1972±0.0006[c]	9.0913±0.0006[d]	9.2116±0.0006[d]	,,
				9.2192±0.0006[d]	,,
				9.2253±0.0008[d]	,,
	8.98±0.01	9.18±0.01	9.10±0.01	9.23±0.01	26
	8.98±0.01	9.17±0.01	9.08±0.01	9.21±0.01	15
	9.09±0.01	9.18±0.01	9.13±0.01	9.23±0.01	17
IE($\tilde{X}_2$)[a]		9.7394±0.0024[b]		9.7847±0.0049[d]	this work
		9.7649±0.0023[c]		9.7877±0.0043[d]	,,
				9.7914±0.0050[d]	,,
				9.7960±0.0039[d]	,,
	9.64±0.01	9.74±0.01	9.68±0.01	9.81±0.01	17
AE($C_4H_9^+$)[e]	9.1762±0.0047	9.643±0.019[f]	9.6466±0.0046	9.7544±0.0045	this work
(0K)	9.180±0.015				19
	9.16±0.03	9.62±0.02	9.55±0.02	9.72±0.02	15
AE($C_4H_9^+$)[e]	8.99±0.01				27
(298K)			9.54±0.01		28
	8.98±0.01				29

[a]$\tilde{X}_1$ and $\tilde{X}_2$ denote lower and upper spin–orbit states, respectively, of the ground electronic state.
[b,c]b and c denote P_H and P_C conformers, respectively. See Fig. 2.
[d]Conformer-specific ionization energies to the lower or upper spin–orbit states.
[e]Appearance energies of $C_4H_9^+$ from iodobutanes at 0 and 298 K.
[f]Determined from photoionization efficiency data.

II. EXPERIMENT

Iodobutanes were purchased from Aldrich and used without further purification. Samples kept at room temperature were seeded in helium or argon carrier gas and expanded into a source vacuum chamber through a 0.5-mm-diameter nozzle orifice (General Valve). The supersonic jet was then skimmed through a 1-mm-diameter skimmer to enter a differentially pumped ionization chamber. The backing pressure was typically 2–3 atmosphere and background pressure of the ionization chamber was maintained below 10^{-7} Torr.

Details of the experimental setup were described previously.[10] Briefly, the second harmonic output of a Nd:YAG laser (Continuum PL8000, 5 ns) was used to pump a dye laser (Continuum ND6000) to generate 649 or 638 nm laser pulses. Then it was frequency-tripled to produce the 216.6 or 212.4 nm output (~0.5 mJ/pulse) which was used to excite the Kr $5p[5/2]_0$-$4p^6$ or $5p[1/2]_0$-$4p^6$ transition via two-photon resonant absorption, respectively. A laser pulse in the 500–700 nm range was also generated by a second dye laser pumped by the 355 or 532 nm output of another Nd:YAG laser. Two laser pulses were then combined and loosely focused by a fused-silica lens (50 cm focal length) prior to entering the Kr gas cell. A MgF_2 lens (20 cm nominal focal length) was placed off-center at the exit of the Kr gas cell to separate the VUV laser output from the input laser pulses in the laser-molecular beam interaction region.[11] The VUV laser in the 125–135 nm region was generated with the Kr pressure optimized in the 1–10 Torr range.

The VUV laser pulse was collinearly overlapped with the molecular beam in a counter-propagation manner, and thus slit-electrodes were used to maximize ion collection efficiency.[12] Spoil field of 0.15–1.0 V/cm was applied, while an electric field of 10–125 V/cm was applied at a certain delay time after the laser pulse for the pulsed-field ionization (PFI) of long-lived ZEKE states. Ions were then accelerated, flied through a field-free region, and were detected by a dual microchannel plate detector. A short pulse of the scrambling field was applied at the laser irradiation time, which lengthened the lifetime of ZEKE states significantly.[10,13] Use of a long delay time (20–40 μs) and low spoil field improved the quality of the MATI spectra tremendously.

III. RESULTS AND DISCUSSION

Since the high PFI field ionizes Rydberg molecules at well below the ionization threshold, ionization energies deduced from MATI spectra are often underestimated from the true values.[14] In the present work, ionization energies to the lower spin–orbit states of molecular ions have been determined by the extrapolation of those deduced from MATI spectra taken at several PFI and spoil fields to the zero-fields via multiple regression. Validity of this method was checked carefully in the previous work.[10] Fragmentation thresholds, however, could not be determined by the above extrapolation method due to low signal levels at low PFI field. Thus, energy calibration factor, deduced by comparing the ionization energies for lower spin–orbit states measured at a particular PFI field with the accurate results, has been used to estimate other values reported here. The values of ionization energies and fragmentation thresholds obtained in this work are compared with previously reported values in Table I.

A. *t*-Butyl iodide

The MATI spectra of *t*-butyl iodide (2-iodo-2-methylpropane) recorded by measuring $C_4H_9I^{+\bullet}$ and its fragment, $C_4H_9^+$, are shown in Fig. 1(a). Observation of $C_4H_9^+$ by PFI means that dissociation has occurred in the ion core

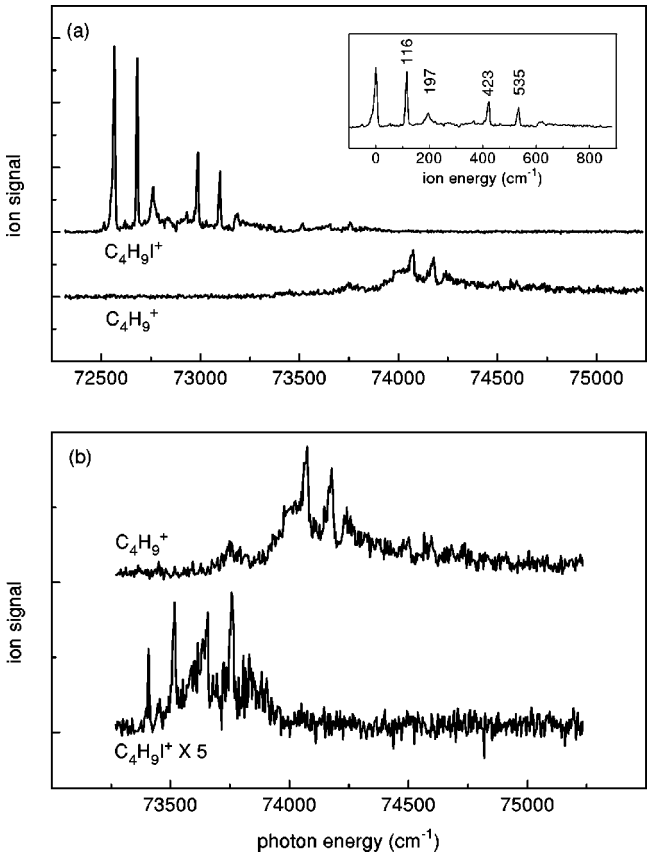

FIG. 1. (a) One-photon VUV MATI spectra of *t*-butyl iodide in the threshold region for ionization to the lower spin–orbit state recorded by monitoring $C_4H_9I^{+\bullet}$ and $C_4H_9^+$ signal. (b) Fragmentation threshold region in (a) is magnified to show the appearance energy determination.

of the neutral in the ZEKE state during the time delay (20–40 μs) between VUV excitation and PFI pulses. Assignment of the major bands in the $C_4H_9I^{+\bullet}$ ion MATI spectrum is rather straightforward because only one conformer exists both for the neutral and molecular ion. Accurate ionization energy to the lower spin–orbit state of *t*-butyl iodide ion can be determined from the position of the first peak in the $C_4H_9I^{+\bullet}$ ion MATI spectrum, which is $72\,577 \pm 5\ \mathrm{cm}^{-1}$ (8.9984 ± 0.0006 eV). This is in reasonable agreement with the previously reported value of 8.98 ± 0.01 eV.[15] Also observed in the MATI spectrum of *t*-butyl iodide are several sharp peaks associated with ionic vibrational energy levels. Comparison with *ab initio* calculation (MP2/LanL2DZ)[16] suggests that the 116, 197, 423, and 535 cm^{-1} bands are due to C-I stretching, C-I bending, C-C bending, and C-I stretching/C-C bending combination, respectively.

According to the photoelectron spectrum,[17] the upper spin–orbit state of t-$C_4H_9I^{+\bullet}$ is located at $\sim 4400\ \mathrm{cm}^{-1}$ above the lower state. Appearance of $C_4H_9^+$ below this energy in Fig. 1(a) means that the fragmentation occurs in the lower state. It is reasonable to assume that the $C_4H_9^+$ fragment has the *tertiary* butyl structure also because it is the most stable among the $C_4H_9^+$ isomers.[18,19] Fragmentation threshold energy can be estimated from the energy where the parent ($C_4H_9I^{+\bullet}$) MATI signal disappears and at the same time the $C_4H_9^+$ fragment MATI signal starts to increase. However, as shown in Fig. 1(b), there exist weak broad bands in the fragment MATI spectrum even below the energy where the parent MATI signal disappears completely. The positions and widths of these peaks in the fragment MATI spectrum do not match with those in the parent MATI spectrum. Thus, possibility of extremely slow reaction (such as tunneling) near the threshold energy can be readily ruled out. Instead, the intensity of the broad bands in the fragment MATI spectrum turned out to be dependent on the molecular beam conditions such as backing pressure or delay time between nozzle-opening event and laser-irradiation. Therefore, the weak broad bands in the fragment MATI spectrum are most likely due to hot-band transition and/or contribution from clusters in the beam. Accordingly, the fragmentation threshold energy has been estimated from the sharp decay of the parent MATI signal, Fig. 1(b), resulting in the appearance energy of $74\,011 \pm 38\ \mathrm{cm}^{-1}$ (9.1762 ± 0.0047 eV) for the $C_4H_9^+$ fragment. This value is in good agreement with the appearance energy of 9.180 ± 0.015 eV measured with PEPICO spectroscopy by Baer and co-workers,[19] Table I. Using the heats of formation data for t-C_4H_9I and I products in the literature,[20,21] $\Delta_f H^0(t\text{-}C_4H_9^+)$ is estimated to be $733.7 \pm 3.3\ \mathrm{kJ\,mol}^{-1}$, which is in agreement with $734 \pm 3.6\ \mathrm{kJ\,mol}^{-1}$ reported previously.[19]

The experimental finding that relatively sharp peaks appear in the $C_4H_9^+$ fragment MATI spectrum even above the fragmentation threshold suggests that both intramolecular vibrational redistribution (IVR) and fragmentation processes are not extremely fast near the fragmentation threshold, namely at $\sim 1400\ \mathrm{cm}^{-1}$ above the zero point level. However, at higher excitation energies the fragment MATI spectrum shows broad and structureless feature, indicating that IVR becomes quite efficient at such energies. Thus the present experimental results are consistent with the general consensus that the fragmentation takes place on the ground ionic state through IVR without an exit barrier.

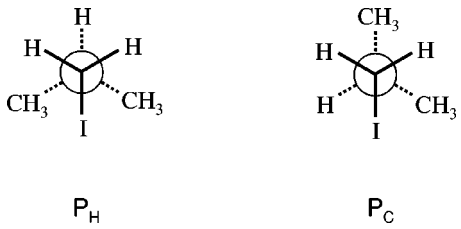

P_H P_C

FIG. 2. Newman projections for the P_H and P_C conformers of *iso*-butyl iodide.

B. *iso*-Butyl iodide

Two conformations with respect to the C(1)-C(2) axis, P_H and P_C, are possible for *iso*-butyl iodide (1-iodo-2-methylpropane),[22] as shown in Fig. 2. Relative thermodynamic stabilities of these two conformers are not accurately known, even though *ab initio* calculation (MP2/LanL2DZ) suggests that the P_C conformer is slightly more stable than the P_H conformer. With the energetics difference between conformers negligible, the population ratio of the

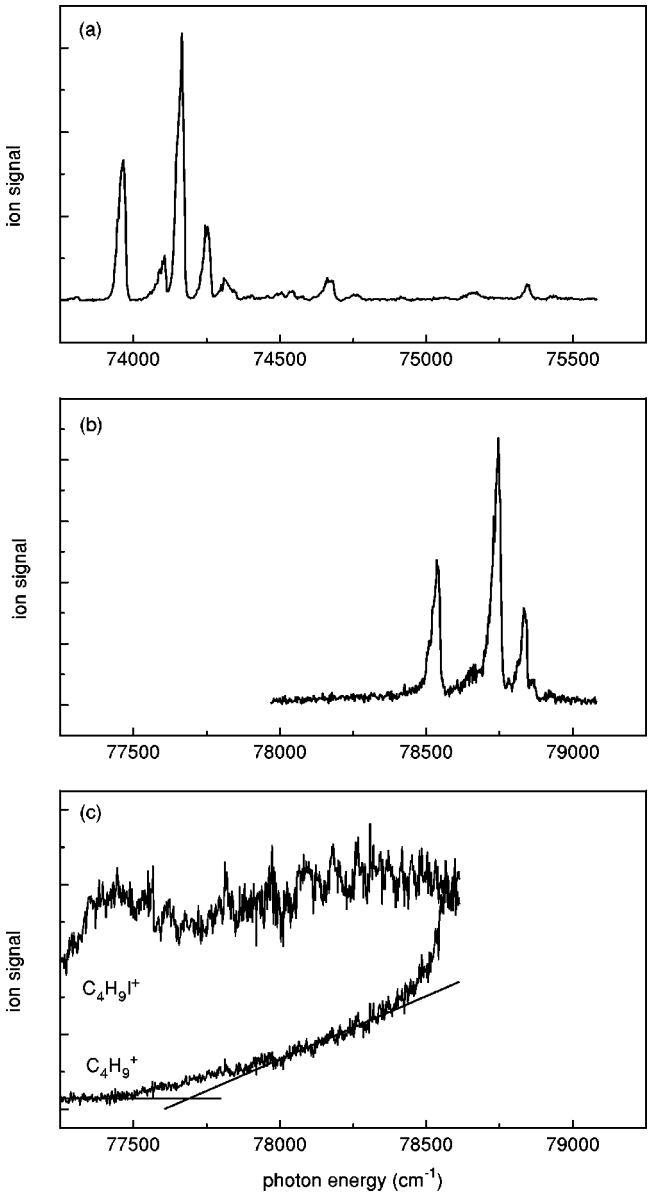

FIG. 3. One-photon VUV MATI spectra of *iso*-butyl iodide recorded by monitoring (a) $C_4H_9I^{+\bullet}$ generated in the lower spin–orbit state and (b) $C_4H_9^+$ generated in the upper spin–orbit state. (c) $C_4H_9I^{+\bullet}$ and $C_4H_9^+$ generated in the fragmentation threshold region in PIE.

P_H and P_C conformers will be mostly determined by the structural degeneracy factor, namely $\sim 1:2$. Assuming that the same ratio holds for the MATI peaks, we assign the peak at $\sim 73\,972\,cm^{-1}$ in the MATI spectrum, Fig. 3(a), to the spectral origin of the P_H conformer ion, while the stronger ($\times 2$) peak at $\sim 74\,171\,cm^{-1}$ is assigned to that of the P_C conformer ion. This means that the ionization energy of P_C is a little higher than that of P_H. The same was found in the *ab initio* calculation at the MP2/LanL2DZ level. Ionization energies of the P_H and P_C conformers of *iso*-butyl iodide determined based on these assignments are $73\,981 \pm 5\,cm^{-1}$ ($9.1725 \pm 0.0006\,eV$) and $74\,180 \pm 5\,cm^{-1}$ ($9.1972 \pm 0.0006\,eV$), respectively. It is to be emphasized that these values are conformer-specific, while all the previous data reported in the literature are the averages over the two conformers. Also to be emphasized is that conformer-specific preparation of $iso\text{-}C_4H_9I^{+\bullet}$ ion beam can be achieved by choosing the wavelength of the VUV radiation used for MATI, as in our previous study on $1\text{-}C_3H_7I$. Several vibrational bands associated with P_H and P_C conformers also appear in Fig. 3(a). *ab initio* calculation at the MP2/LanL2DZ level predicts two C-I bending frequencies at 71 and $142\,cm^{-1}$ for the P_H conformer ion and at 77 and $138\,cm^{-1}$ for the P_C conformer ion. Thus, the peak at $\sim 74\,106\,cm^{-1}$ can be assigned to C-I bending of the P_H conformer, while those at $\sim 74\,261$ and $\sim 74\,319\,cm^{-1}$ to the two C-I bending modes of the P_C conformer. Assignment of other bands is rather ambiguous and has not been attempted.

Ionization energies of the P_H and P_C conformers to their upper spin–orbit states could be determined from the MATI spectrum recorded by monitoring the $C_4H_9^+$ signal, Fig. 3(b). Spectral pattern of this spectrum is very similar to that of the lower spin–orbit state MATI [Fig. 3(a)] and hence the conformational assignment is straightforward. The ionization energies to the upper spin–orbit states based on these assignments are $78\,554 \pm 19\,cm^{-1}$ ($9.7394 \pm 0.0024\,eV$) and $78\,759 \pm 19\,cm^{-1}$ ($9.7649 \pm 0.0023\,eV$) for P_H and P_C conformers, respectively. No MATI signal due to the parent ion is observed in the same energy region, which indicates that fragmentation threshold is located below the upper spin–orbit state origins. It was difficult to measure the parent ion MATI signal near the fragmentation threshold region. Instead, photoionization efficiency (PIE) curve for the $C_4H_9^+$ fragment was measured, Fig. 3(c), and its appearance energy was deduced from the data. The appearance energy of $77\,770 \pm 150\,cm^{-1}$ ($9.643 \pm 0.019\,eV$) thus obtained compares well with the previously reported value of $9.62 \pm 0.02\,eV$.[15] The fragmentation threshold is located below the upper spin–orbit state origins by $\sim 780\,cm^{-1}$.

The upper spin–orbit state origins correspond to the excess energy of $\sim 4570\,cm^{-1}$ from the lower spin–orbit state origins. The vibrational state density of the lower spin–orbit states is estimated to be around $4 \times 10^4/cm^{-1}$ at this energy. Accordingly, if the upper spin–orbit states are strongly coupled to dissociative dark states in the lower spin–orbit states, spectral congestion or peak broadening is expected in the $C_4H_9^+$ fragment MATI spectrum. However, the spectrum, Fig. 3(b), is found to be quite simple and the widths of individual peaks are almost the same as those due to the lower spin–orbit states in the parent ion MATI spectrum, Fig. 3(a). Therefore, similar to the fragmentation of 1-iodopropane ion,[10] the upper-to-lower spin–orbit state transition may act as the dynamic bottleneck in the dissociation of *iso*-butyl iodide ion in the upper spin–orbit state to $C_4H_9^+ + I$.

C. 2-Iodobutane

Three conformations with respect to the C(2)-C(3) axis, *A*, *G*, and *G′*, are possible for 2-iodobutane, Fig. 4. It is well known from the vibrational spectroscopy of the 2-substituted butane derivatives that the *G′* conformer is the least stable of the three.[23] Two peaks appear distinctly at $\sim 73\,292$ and $\sim 73\,316\,cm^{-1}$ in the MATI spectrum of 2-iodobutane in Fig. 5(a). One possible assignment is to take the lower frequency peak as the origin and the higher fre-

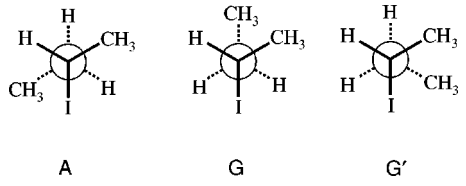

FIG. 4. Newman projections for the *A*, *G*, and *G′* conformers of 2-iodobutane.

quency one as the vibrationally excited band. This is not likely because the latter is separated from the former only by $\sim 24\,\mathrm{cm}^{-1}$ and is more intense than the former. A more plausible assignment is to take both of these as the origin bands for the *A* and *G* conformers. Still, it is a formidable task to determine which is which. We will just mention here that our attempt to conformer-assign these bands through *ab initio* calculation was fruitless. Even though the conformer assignment could not be done, we determined the ionization energies to the lower spin–orbit states, which were $73\,302 \pm 5\,\mathrm{cm}^{-1}$ ($9.0883 \pm 0.0006\,\mathrm{eV}$) and $73\,326 \pm 5\,\mathrm{cm}^{-1}$ ($9.0913 \pm 0.0006\,\mathrm{eV}$). These are in good agreement with $9.08 \pm 0.01\,\mathrm{eV}$ reported by Baer and co-workers,[15] Table I.

The MATI spectra probing the parent ion or $C_4H_9^+$ fragment do not show any sharp feature in the threshold region to the upper spin–orbit state. Rather, only broad and structureless bands are observed in both MATI spectra as shown in Fig. 5(b). Consequently, ionization energies to the upper spin–orbit states of 2-iodobutane ion could not be precisely determined. Instead, sharp decrease of the parent MATI signal is observed at $\sim 77\,795\,\mathrm{cm}^{-1}$, indicating that the fragmentation of 2-iodobutane ion is nearly complete within $\sim 20\,\mu\mathrm{s}$ at this energy. The ionization energy to the upper spin–orbit state was previously measured to be $9.68 \pm 0.01\,\mathrm{eV}$ ($\sim 78\,100\,\mathrm{cm}^{-1}$) by PES.[17] Therefore, it is very likely that the fragmentation threshold is lower than the upper spin–orbit state origin. However, the threshold energy could not be determined from the MATI spectra unambiguously. While the parent MATI signal disappears completely at $\sim 77\,795\,\mathrm{cm}^{-1}$, the $C_4H_9^+$ MATI signal starts to appear at much lower energy of $\sim 77\,420\,\mathrm{cm}^{-1}$, Fig. 5(b). Two explanations are possible. One is to assume the involvement of hot-band transitions, which may allow the fragment to appear below the true threshold energy. The other possibility is that the fragmentation occurs very slowly in the threshold region such that MATI signals for the parent and fragment coexist even after a long delay time of $\sim 20\,\mu\mathrm{s}$ after the laser pulse. The appearance energy of the $C_4H_9^+$ fragment was previously measured to be $9.55 \pm 0.02\,\mathrm{eV}$ by PEPICO spectroscopy[15] and is closer to the appearance energy estimated from the fragment MATI signal. Hence, it may be tempting to adopt the second of the explanations above, namely very slow dissociation near the threshold. The broad structureless bands in MATI spectra in Fig. 5(b) indicate that state-mixing is nearly complete in the lower spin–orbit state at the excess energy of $\sim 4500\,\mathrm{cm}^{-1}$. This, in turn, suggests that the reaction near the threshold may occur statistically and its rate constant may be reasonably estimated by the Rice–Ramsperger–Kassel–Marcus (RRKM) theory.[24] The vibrational frequencies for the *A* conformer ion obtained by *ab initio* calculation (MP2/LanL2DZ) and the threshold energy of $4250\,\mathrm{cm}^{-1}$ estimated from the appearance of the fragment ion signal in Fig. 5(b) were used in the RRKM calculation. The rate constant at the threshold thus estimated was $2.6 \times 10^6\,\mathrm{s}^{-1}$. The calculated rate constant is larger, by nearly two orders of magnitude, than needed to validate the slow dissociation model. An alternative may be that fragmentation occurs via tunneling at the threshold region through an exit barrier. We do not have any information to clarify the situation. Hence, we take tentatively the threshold determined from the sharp decrease of the parent MATI signal as the appearance energy of the $C_4H_9^+$ fragment, Table I. To unravel the nature of this ion-core dissociation, real-time rate measurement would be desirable.

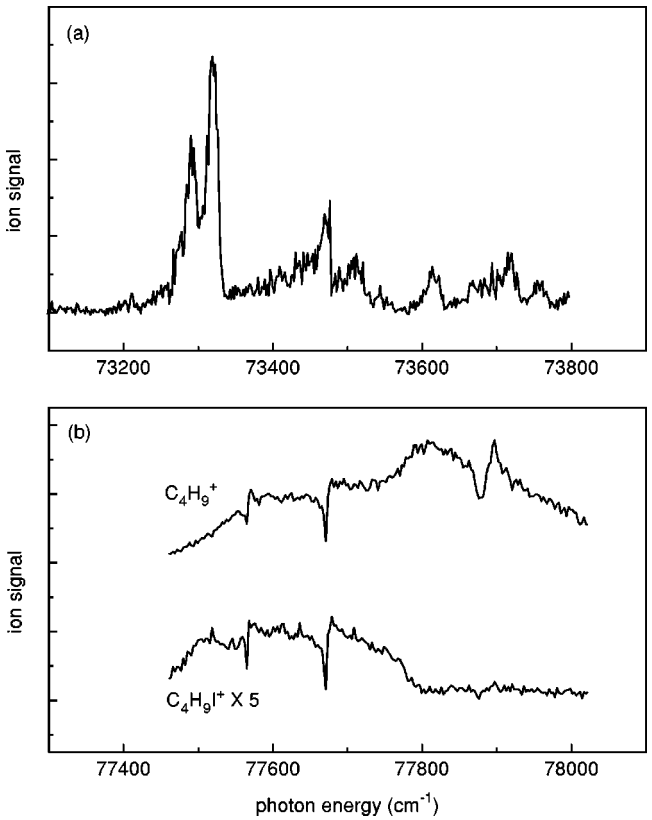

FIG. 5. One-photon VUV MATI spectra of 2-iodobutane. (a) $C_4H_9I^{+\bullet}$ generated in the lower spin–orbit state and (b) $C_4H_9I^{+\bullet}$ and $C_4H_9^+$ generated in the fragmentation threshold region.

D. 1-Iodobutane

Conformational isomerism for this molecule is more complicated than the aboves because not only the conformations around the C(2)-C(3) axis but those around the C(1)-C(2) axis must be taken into account. Total of five conformers are possible, *AA*, *GA*, *AG*, *GG*, and *GG′* in Fig. 6. According to the electron diffraction study,[25] only three of these five are significantly populated in the gas phase at $23°C$; *AA* ($19 \pm 17\%$), *GA* ($17 \pm 31\%$), and *GG* ($64 \pm 31\%$). On the other hand, four bands appear distinctly in the ionization threshold region, namely at $\sim 74\,261$, $\sim 74\,286$, $\sim 74\,343$, and $\sim 74\,400\,\mathrm{cm}^{-1}$, of the MATI spec-

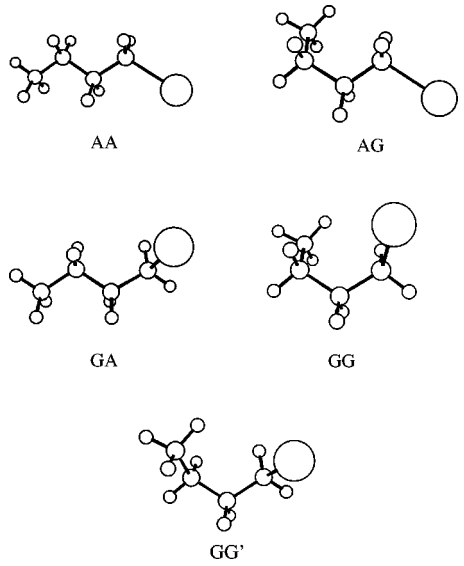

FIG. 6. Structures of *AA*, *GA*, *AG*, *GG*, and *GG′* conformers of 1-iodobutane.

trum of 1-iodobutane, Fig. 7(a). Accepting the results from the above electron diffraction study, one of these may be due to the contribution from the vibrationally excited neutral, clusters, or vibrational excitation in the molecular ion. Since the situation is very complicated, we will not make any attempt to identify these bands. Ionization energies associated with these four bands are listed in Table I.

The appearance energy of the $C_4H_9^+$ fragment from 1-iodobutane has been determined to be 78 674 $\pm 36\,cm^{-1}$ (9.7544 ± 0.0045 eV) from the disappearance of the parent MATI signal, Fig. 7(c). This is in good agreement with 9.72 ± 0.02 eV measured previously by PEPICO spectroscopy.[15] Figure 7(b) shows the fragment ion MATI spectrum near the upper spin–orbit state region. Compared to the lower spin–orbit state spectrum in Fig. 7(a), bands in this spectrum are much broader and separations are smaller. Through repeated measurements, we could confirm the presence for four bands at around ~78 911, ~78 932, ~78 959, and ~79 003 cm^{-1}, which may correspond to four conformers observed in the lower spin–orbit state region. The ionization energies to the upper spin–orbit state of 1-iodobutane estimated from these bands are $78\,919 \pm 40\,cm^{-1}$ (9.7847 ± 0.0049 eV), $78\,943 \pm 35\,cm^{-1}$ (9.7877 ± 0.0043 eV), $78\,973 \pm 40\,cm^{-1}$ (9.7914 ± 0.0050 eV), and 79 010 $\pm 31\,cm^{-1}$ (9.7960 ± 0.0039 eV). These are in good agreement with the average ionization energy of 9.81 ± 0.01 eV determined previously by photoelectron spectroscopy.[17]

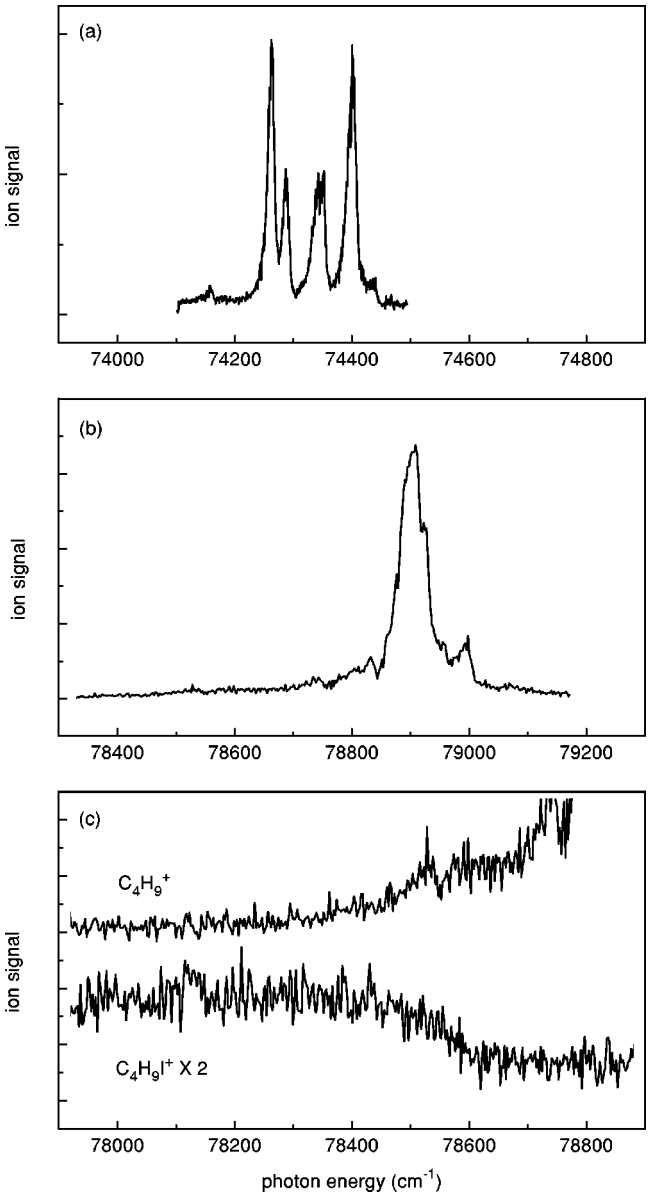

FIG. 7. One-photon VUV MATI spectra of 1-iodobutane. (a) $C_4H_9I^{+\bullet}$ generated in the lower spin–orbit state, (b) $C_4H_9^+$ generated in the upper spin–orbit state, and (c) $C_4H_9I^{+\bullet}$ and $C_4H_9^+$ generated in the fragmentation threshold region.

IV. CONCLUSION

Overall, ionization energies and fragmentation threshold energies of iodobutane isomers determined by MATI spectroscopy in this work have been found to be in reasonably good agreement with previously reported values determined by PES, PIE, or PEPICO spectroscopy. However, the values determined here are more precise and probably more accurate. Furthermore, it is to be emphasized that the values associated with ionization are now conformer-specific. As has been demonstrated in our earlier work on 1-iodopropane, a beam of a particular conformer of *iso*-butyl iodide, 2-iodobutane, or 1-iodobutane ions can be now selectively prepared by just tuning the excitation VUV wavelength. Fragmentation of 2-iodobutane ion in the upper spin–orbit state occurs via efficient coupling to dissociative dark states in the lower spin–orbit state. On the other hand, the upper-to-lower spin–orbit state transition may act as the dynamical bottleneck in the fragmentation of *iso*-butyl iodide ion in the upper spin–orbit state. 1-iodobutane ion may lie half way between these two in terms of the efficiency of the upper-to-lower spin–orbit state transition. In conclusion, we have here investigated the ionization and ion-core fragmentation of various isomers of iodobutane. The way how alkyl groups are chemically arranged around the formal charge center of the molecular ion has turned out to affect both ionization and

fragmentation energetics significantly. A highlight of this work may be that a new method has been developed which can be used to investigate the conformational effect on spectroscopy and dynamics of iodobutane ions. In particular, capability to study conformer-specific chemical processes may lead to better understanding of the influence of conformation on reaction dynamics which has been an important subject in organic chemistry over the years.

ACKNOWLEDGMENTS

This work was supported financially by CRI, the Ministry of Science and Technology, Republic of Korea. S. T. Park thanks the Ministry of Education, Republic of Korea, for the financial support through the Brain Korea 21 program.

[1] K. Müller-Dethlefs, M. Sander, and E. W. Schlag, Chem. Phys. Lett. **112**, 291 (1984).
[2] I. Fischer, R. Lindner, and K. Müller-Dethlefs, J. Chem. Soc., Faraday Trans. **90**, 2425 (1994).
[3] K. Müller-Dethlefs and E. W. Schlag, Annu. Rev. Phys. Chem. **42**, 109 (1991).
[4] E. W. Schlag, *ZEKE Spectroscopy* (Cambridge University Press, Cambridge, 1998).
[5] J. W. Hepburn, Chem. Soc. Rev. **25**, 281 (1996).
[6] L. Zhu and P. Johnson, J. Chem. Phys. **94**, 5769 (1991).
[7] H. Krause and H. J. Neusser, J. Chem. Phys. **97**, 5923 (1992).
[8] R. Hilbig, A. Lago, and R. Wallenstein, J. Opt. Soc. Am. B **4**, 1753 (1983).
[9] J. P. Marangos, N. Shen, H. Ma, M. H. R. Hutchinson, and J. P. Connerade, J. Opt. Soc. Am. B **7**, 1254 (1990).
[10] S. T. Park, S. K. Kim, and M. S. Kim, J. Chem. Phys. **114**, 5568 (2001).
[11] S. A. Meyer and G. W. Faris, Opt. Lett. **23**, 204 (1998).
[12] E. Nir, H. E. Hunziker, and M. S. De Vries, Anal. Chem. **71**, 1674 (1999).
[13] (a) A. Held, U. Aigner, L. Y. Baranov, H. L. Selzle, and E. W. Schlag, Chem. Phys. Lett. **299**, 110 (1999); (b) A. Held, L. Y. Baranov, H. L. Selzle, and E. W. Schlag, *ibid.* **291**, 318 (1998); (c) A. Held, H. L. Selzle, and E. W. Schlag, J. Phys. Chem. **100**, 15314 (1996).
[14] R. Lindner, H. Dietrich, and K. Müller-Dethlefs, Chem. Phys. Lett. **228**, 417 (1994).
[15] M. C. Oliveira, T. Baer, S. Olesik, and M. A. A. Ferreira, Int. J. Mass Spectrom. Ion Processes **82**, 299 (1988).
[16] M. J. Frisch, G. W. Trucks, H. B. Schlegel *et al.*, Gaussian 98, Revision A.6, Gaussian, Inc., Pittsburgh, PA, 1998.
[17] K. Kimura, S. Katsumata, Y. Achiba, T. Yamazaki, and S. Iwata, *Handbook of HeI Photoelectron Spectra of Fundamental Organic Molecules* (Japan Scientific Societies Press, Tokyo, 1981).
[18] C. Aubry and J. L. Holmes, J. Phys. Chem. A **102**, 6441 (1998).
[19] J. W. Keister, J. S. Riley, and T. Baer, J. Am. Chem. Soc. **115**, 12613 (1993).
[20] J. B. Pedley, R. D. Naylor, and S. P. Kirby, *Thermochemical Data of Organic Compounds*, 2nd ed. (Chapman and Hall, London, 1986).
[21] D. D. Wagman, W. H. E. Evans, V. B. Parker, R. H. Schum, I. Halow, S. M. Mailey, K. L. Churney, and R. L. Nuttall, The NBS Tables of Chemical Thermodynamic Properties, in J. Phys. Chem. Ref. Data **11**, Suppl. 2 (1982).
[22] (a) J. R. Durig, J. F. Sullivan, and S. E. Godbey, J. Mol. Struct. **146**, 213 (1986); (b) G. A. Crowder and W. Lin, *ibid.* **64**, 193 (1980).
[23] E. Benedetti and P. Cecchi, Spectrochim. Acta, Part A **28**, 1007 (1972).
[24] K. A. Holbrook, M. J. Pilling, and S. H. Robertson, *Unimolecular Reactions*, 2nd ed. (Wiley, New York, 1996).
[25] K. Aarset, K. Hagen, R. Stølevik, and P. C. Sæbø, Struct. Chem. **6**, 197 (1995).
[26] Gas Phase Ion Energetics, in *NIST Chemistry WebBook: NIST Standard Reference Database 69* [Natl. Inst. Standards and Tech. (http://webbook.nist.gov), Gaithersburg, MD, 1998].
[27] J. C. Traeger, Rapid Commun. Mass Spectrom. **10**, 119 (1996).
[28] J. C. Traeger and R. G. McLoughlin, J. Am. Chem. Soc. **103**, 3647 (1981).
[29] R. G. McLoughlin and J. C. Traeger, J. Am. Chem. Soc. **101**, 5791 (1979).